# On the Magnification Relations in Quadruple Lenses: A Moment Approach

Hans J. Witt¹★ Shude Mao²†

<sup>1</sup> Astrophysikalisches Institut Potsdam, An der Sternwarte 16, 14482 Potsdam, Germany

<sup>2</sup>Max-Planck-Institute für Astrophysik, Karl-Schwarzschild-Strasse 1, 85740 Garching, Germany

Accepted ....... Received ......; in original form ......

#### ABSTRACT

We present a new method of studying quadruple lenses in elliptical power-law potentials parameterized by  $\psi(x,y) \propto (x^2 + y^2/q^2)^{\beta/2}/\beta$  ( $0 \le \beta < 2$ ). For this potential, the moments of the four image positions weighted by signed magnifications (magnification times parity) have very simple properties. In particular, we find that the zeroth moment – the sum of four signed magnifications satisfies  $\simeq 2/(2-\beta)$ ; the relation is exact for  $\beta=0$  (point-lens) and  $\beta=1$  (isothermal potential), independent of the axial ratio. Similar relations can be derived when a shear is present along the major or minor axes. These relations, however, do not hold well for the closely-related elliptical density distributions. For a singular isothermal elliptical density distribution without shear, the sum of signed magnifications for quadruple lenses is  $\approx 2.8$ , again nearly independent of the ellipticity. For the same distribution with shear, the total signed magnification is around 2-3 for most cases, but can be significantly different for some combinations of the axial ratio and shear where more than four images can appear.

**Key words:** galactic structure – gravitational lensing

<sup>\*</sup> e-mail: hwitt@aip.de

<sup>†</sup> e-mail: smao@mpa-garching.mpg.de

#### 2 Witt & Mao

#### 1 INTRODUCTION

Since the discovery of the first double lens 0957+0561 by Walsh, Carswell & Weymann (1979), gravitational lensing has found many cosmological applications (see Schneider, Ehlers & Falco 1992; Narayan & Bartelmann 1998 and references therein). One of these applications is to probe the potential of lensing galaxies in multiply-imaged quasars. In this aspect, the quadruple lenses are ideal systems since they provide more constraints than the double lenses. Previous modelings of these systems use mainly isothermal elliptical potentials and their variants (e.g., Kochanek 1991; Keeton, Kochanek & Seljak 1997; Witt, Mao & Schechter 1995). In many of these modelings, attention was paid only to the image positions with a few exceptions, which considered the flux ratios (e.g., Keeton, Kochanek & Seljak 1997). Since optical flux ratios are likely to be influenced by microlensing (Chang & Refsdal 1979), they should be used with care. On the other hand, radio fluxes should be nearly unaffected by microlensing since the radio emission regions are believed to have larger sizes (there are exceptions for very highly magnified systems such as B1422+231, see Mao & Schneider 1998). Satisfactory lens models should ideally fit the image positions as well as the flux ratios. However, previous numerical studies often find it very difficult to fit these with isothermal potentials and their variants (e.g., Keeton, Kochanek & Seljak 1997). The purpose of this paper is two-fold: first we extend the isothermal potentials to a more general class of power-law potentials and uncover some generic scaling relations. The three-dimensional correspondence of this class of potential provide a reasonable analytical approximation to the galactic potential (Evans 1994). Second, we study the relations for related isothermal elliptical density distributions and show that there are qualitative and quantitative differences between elliptical density and elliptical potential distributions.

The outline of the paper is as follows. In §2, we introduce the elliptical power-law potentials and derive some scaling relations with a new moment approach. In §3, we study the singular isothermal elliptical density distribution with arbitrary shear to understand the difference between these two types of potentials. In §4, we summarize and discuss the implications of our results for lens modeling.

#### 2 ELLIPTICAL POWER-LAW POTENTIAL

In this section we study elliptical power-law potentials as models for lensing galaxies. This potential form is widely used in gravitational lensing (e.g., Blandford & Kochanek 1987;

Kassiola & Kovner 1993 and references therein). It is easier to study than the more realistic but more complex elliptical density distribution (e.g., Kormann, Schneider & Bartelmann 1994; Hogg & Blandford 1994; Chae, Khersonsky, & Turnshek 1998); we return to the elliptical density distributions in §3.

The power-law potential is given by

$$\psi(x,y) = a \frac{(x^2 + y^2/q^2)^{\beta/2}}{\beta} \quad \text{for} \quad 0 < \beta < 2$$
 (1)

$$\psi(x,y) = a \frac{\ln(x^2 + y^2/q^2)}{2} \quad \text{for} \quad \beta = 0$$
 (2)

where q (0 <  $q \le 1$ ) is the axial ratio of the lensing galaxy,  $\beta$  the slope of the potential and a determines the overall strength of the lens system. The coordinate system has been chosen such that the center of the lensing galaxy is at the origin and the major axis of the galaxy is along the x-axis. In general the orientation of the major axis of the lensing galaxy is unknown, but can be easily determined if the image configurations can be modeled by an elliptical potential (Witt 1996). Note that the point-mass potential is described by  $\beta = 0, q = 1$ , the elliptical isothermal sphere by  $\beta = 1$ , and the constant surface mass distribution by  $\beta \to 2, q = 1$ . Thus the commonly used potentials in numerical modeling are all special cases of this class.

#### 2.1 Lens equation

The lens equation for the power-law potential is given by

$$\xi = x - \frac{ax}{(x^2 + y^2/q^2)^{1-\beta/2}},\tag{3}$$

$$\eta = y - \frac{ayq^{-2}}{(x^2 + y^2/q^2)^{1-\beta/2}}. (4)$$

It is easy to show that the lens equation with an *on-axis* shear can be transformed into eqs. (3) and (4) with suitable coordinate transformations as given in §2.5. So with small modifications our results apply to the case with an on-axis shear as well (§2.5). Notice that the elliptical potentials (including the special power-law form studied here) restrict the image and galaxy positions to be located on a hyperbolic line (Witt 1996). Image configurations which do not follow these constraints require far more complicated lens models, in particular may require an off-axis shear (Keeton, Kochanek & Seljak 1997; Witt & Mao 1997).

## **2.2** Exact relations for $\beta = 1$ and $\beta = 0$

Although the lens equations (3) and (4) are in general too complicated to solve for the image positions and the magnifications, here we present a new method to directly relate the image magnification and positions to the properties of the galaxy potential. The new method is similar to the Jeans equation in galactic dynamics (e.g., Binney & Tremaine 1987, p. 195). It is possible to extend this new technique to other potential forms such as that for binary lens. However, in the latter case, the application may be limited since in microlensing we can not resolve the individual images. In the next subsection, we illustrate our technique using an isothermal ( $\beta = 1$ ) elliptical potential; in §2.3, we discuss the case for  $\beta = 0$ .

## 2.2.1 Isothermal elliptical potential ( $\beta = 1$ )

There are different ways to derive relationships between the image positions and their magnifications. Sometimes it is more convenient to use the complex formalism (cf. Rhie 1997 for the binary lens application) or the resultant method (e.g., Witt & Mao 1995; Dalal 1998). Here we adopt a general analytical approach using real quantities. When a source is inside the inner caustic of an elliptical potential, there are always four images. The lens equation (3) or (4) can be manipulated into two polynomials of degree 4 of separated arguments in x and y:

$$g_x(x,\xi,\eta) = \sum_{n=0}^{4} a_n x^n = a_4 \prod_{i=1}^{4} (x - x_i), \quad g_y(y,\xi,\eta) = \sum_{n=0}^{4} b_n y^n = b_4 \prod_{i=1}^{4} (y - y_i)$$
 (5)

where  $(x_i, y_i)$  are the coordinates of the *i*-th image, and the polynomial coefficients are given by

$$a_4 = (1 - q^2)^2, b_4 = q^2(1 - q^2)^2,$$
 (6)

$$a_3 = 2\xi(1-q^2)(q^2-2), \quad b_3 = 2\eta q^2(1-q^2)(2q^2-1),$$
 (7)

$$a_2 = -a^2(1-q^2)^2 + 6\xi^2(1-q^2) + q^2(q^2\xi^2 + \eta^2)$$
  $b_2 = a_2 - 6(\eta^2q^4 + \xi^2)(1-q^2)$  (8)

$$a_1 = 2\xi[a^2(1-q^2) - 2\xi^2 + q^2(\xi^2 - \eta^2)[$$
  $b_1 = -2q^2\eta[a^2(1-q^2) + 2q^4\eta^2 + q^2(\xi^2 - \eta^2)]$  (9)

$$a_0 = -\xi^2 [a^2 - (\xi^2 + q^2\eta^2)], \quad b_0 = -\eta^2 q^4 [a^2 - (\xi^2 + q^2\eta^2)]$$
 (10)

The Jacobian matrix for the mapping from the lens plane to the image plane is defined as

$$J = \begin{pmatrix} \frac{\partial \xi}{\partial x} & \frac{\partial \xi}{\partial y} \\ \frac{\partial \eta}{\partial x} & \frac{\partial \eta}{\partial y} \end{pmatrix} \tag{11}$$

For each image, there is a one-to-one inverse mapping from the image plane to the lens plane,

$$J^{-1} = \begin{pmatrix} \frac{\partial x}{\partial \xi} & \frac{\partial x}{\partial \eta} \\ \frac{\partial y}{\partial \xi} & \frac{\partial y}{\partial \eta} \end{pmatrix} = \frac{1}{\det J} \begin{pmatrix} \frac{\partial \eta}{\partial y} & -\frac{\partial \xi}{\partial y} \\ -\frac{\partial \eta}{\partial x} & \frac{\partial \xi}{\partial x} \end{pmatrix}, \tag{12}$$

where the second equality comes from the conventional definition of an inverse matrix. A comparison of the diagonal elements gives

$$\frac{\partial y}{\partial \eta} = \frac{1}{\det J} \frac{\partial \xi}{\partial x}, \quad \frac{\partial x}{\partial \xi} = \frac{1}{\det J} \frac{\partial \eta}{\partial y} \tag{13}$$

The sum of the two expressions is

$$\frac{\partial y}{\partial \eta} + \frac{\partial x}{\partial \xi} = \frac{1}{\det J} \left[ \frac{\partial \xi}{\partial x} + \frac{\partial \eta}{\partial y} \right] = \frac{1}{\det J} + 1, \tag{14}$$

where we have used

$$\frac{\partial \xi}{\partial x} + \frac{\partial \eta}{\partial y} = 1 + \det J \quad \text{for} \quad \beta = 1. \tag{15}$$

The signed magnification for a given image is by definition

$$p_i \mu_i \equiv \frac{1}{\det J} \Big|_{(x_i, y_i)} = \frac{\partial y_i}{\partial \eta} + \frac{\partial x_i}{\partial \xi} - 1, \tag{16}$$

where  $\mu_i$  is the absolute magnification for a given image,  $p_i = \pm 1$  is the parity of the images, and we substituted det J from eq. (14).

Now the sum of signed magnifications is then

$$\sum_{i=1}^{4} p_i \mu_i = \frac{\partial}{\partial \xi} \sum_{i=1}^{4} x_i(\xi, \eta) + \frac{\partial}{\partial \eta} \sum_{i=1}^{4} y_i(\xi, \eta) - 4 = \frac{\partial}{\partial \xi} \left( -\frac{a_3}{a_4} \right) + \frac{\partial}{\partial \eta} \left( -\frac{b_3}{b_4} \right) - 4. \tag{17}$$

In the second step we have used the fact that the sum of the roots of a polynomial is related to its coefficients. Using the coefficients as given in eqs. (6) to (10), we obtain

$$\sum_{i=1}^{4} p_i \mu_i = 2. (18)$$

A similar relation was found recently by Dalal (1998) for  $\beta = 1$ . This implies that for an isothermal elliptical potential the signed magnification is always 2, independent of the axial ratio and the image configurations.

Using similar techniques, we can calculate higher order moments of positions, defined as

$$\mathcal{M}_{n,x} \equiv \sum_{i=1}^{4} p_i \mu_i x_i^n, \quad \mathcal{M}_{n,y} \equiv \sum_{i=1}^{4} p_i \mu_i y_i^n$$
(19)

For illustration, we derive the x-component of the first moment:

$$\mathcal{M}_{1,x} = \sum_{i=1}^{4} p_i \mu_i x_i = \sum_{i=1}^{4} \left[ \frac{\partial y_i}{\partial \eta} + \frac{\partial x_i}{\partial \xi} - 1 \right] x_i, \tag{20}$$

where in the second equality we have again used eq. (14). Changing now the order of summation and derivation, and using the fact that the Jacobian matrix is symmetric  $(\partial y/\partial \xi = \partial x/\partial \eta)$ , we obtain:

$$\sum_{i=1}^{4} p_i \mu_i x_i = \frac{1}{2} \frac{\partial}{\partial \xi} \sum_{i=1}^{4} (x_i^2 - y_i^2) + \frac{\partial}{\partial \eta} \sum_{i=1}^{4} x_i y_i - \sum_{i=1}^{4} x_i$$
(21)

For the first and third terms we can easily replace the sum by expressions of the coefficients of the polynomial:

$$\sum_{i=1}^{4} x_i^2 = \frac{a_3^2 - 2a_2 a_4}{a_4^2}, \quad \sum_{i=1}^{4} y_i^2 = \frac{b_3^2 - 2b_2 b_4}{b_4^2}, \quad \text{and} \quad \sum_{i=1}^{4} x_i = -\frac{a_3}{a_4}. \tag{22}$$

For the second mixed term in x and y of eq. (21), we recall that for any elliptical potential, the x and y components for a given image are related (cf. eqs. [3] and [4]) by:

$$\frac{\xi - x_i}{\eta - y_i} = q^2 \frac{x_i}{y_i}, \text{ thus } y_i = \frac{\eta q^2 x_i}{\xi - x_i (1 - q^2)}$$
 (23)

Now the mixed term can be written as

$$\sum_{i=1}^{4} x_i y_i = \frac{\eta q^2}{1 - q^2} \sum_{i=1}^{4} \frac{x_i^2}{\xi/(1 - q^2) - x_i} 
= \frac{\eta q^2}{1 - q^2} \left[ \frac{a_3}{a_4} - \frac{4\xi}{1 - q^2} + \frac{\xi^2}{(1 - q^2)^2} \sum_{i=1}^{4} \frac{1}{\xi/(1 - q^2) - x_i} \right]$$
(24)

where we have expressed the mixed term in terms of a sum of different powers of  $x_i$ . The last term in the previous equation can be expressed in terms of the polynomial:

$$\sum_{i=1}^{4} \frac{1}{x - x_i} \Big|_{x = \xi/(1 - q^2)} = \frac{1}{g_x(x, \xi, \eta)} \frac{dg_x(x, \xi, \eta)}{dx} = \frac{2(1 - q^2)}{\xi q^2}$$
 (25)

Collecting all terms together, we obtain

$$\sum_{i=1}^{4} p_i \mu_i x_i = 2\xi, \quad \sum_{i=1}^{4} p_i \mu_i y_i = 2\eta, \tag{26}$$

a remarkably simple result. Higher order moments can be obtained similarly and are summarized in §2.4. However, first we discuss results for another special case with  $\beta = 0$ .

## **2.3** Point lens $(\beta = 0)$

For  $\beta = 0$ , the potential approximates a point lens plus shear. It is easy to separate the lens equations into two polynomials of degree 4 for x and y – We only have to insert eq. (23) into the lens equations (3) and (4). Therefore we do not present the coefficients here. The derivations for magnification moments are similar, except that eq. (14) must be changed. To do this, we notice that for  $\beta = 0$ , we have

$$\frac{\partial \xi}{\partial x} + q^2 \frac{\partial \eta}{\partial y} = 1 + q^2. \tag{27}$$

Using eq. (13), we obtain

$$\frac{\partial y}{\partial \eta} + q^2 \frac{\partial x}{\partial \xi} = \frac{1}{\det J} \left[ \frac{\partial \xi}{\partial x} + q^2 \frac{\partial \eta}{\partial y} \right] = \frac{1 + q^2}{\det J}.$$
 (28)

In the last step, we have expressed the signed magnification  $(\mu_i p_i = 1/\det J)$  in terms of  $\partial y/\partial \eta$  and  $\partial x/\partial \xi$ , similar to the case for  $\beta = 1$ . The rest of derivation proceeds nearly identically. For the zeroth and first moments we have

$$\sum_{i=1}^{4} \mu_i p_i = 1, \quad \sum_{i=1}^{4} p_i \mu_i x_i = \xi, \quad \sum_{i=1}^{4} p_i \mu_i y_i = \eta, \tag{29}$$

### 2.4 Relations for more general power-law potentials

For more general cases with non-integer values between 0 and 2, there is no simple way to derive analogous relations. However, the special cases for  $\beta = 0$  and  $\beta = 1$  suggests approximation by interpolation. In particular,

$$\sum_{i=1}^{4} \mu_i p_i \simeq B, \quad B \equiv \frac{2}{2-\beta}. \tag{30}$$

For  $\beta = 0$  and  $\beta = 1$ , eq. (30) is exact. For other non-integer values, this equation is only approximate, but we find numerically that it is valid to  $\lesssim 5\%$ . Therefore, for an quadruple lens well-modeled by power-law elliptical potentials, this relation is approximately valid, independent of the source position. A similar exact relation is also satisfied by the binary lens, where the sum of signed magnifications of five image cases is equal to 2 (Witt & Mao 1995; Rhie 1997).

Starting from eq. (30), we can obtain moment equations that relate the image positions and magnifications to the parameters of the potential.

$$\sum_{i=1}^{4} \mu_i p_i x_i = B\xi, \quad \sum_{i=1}^{4} \mu_i p_i y_i = B\eta, \tag{31}$$

$$\sum_{i=1}^{4} \mu_i p_i x_i^2 = -A + B\xi^2, \quad \sum_{i=1}^{4} \mu_i p_i y_i^2 = Aq^{-2B} + B\eta^2, \tag{32}$$

$$\sum_{i=1}^{4} \mu_i p_i x_i^3 = -A\xi (B + \frac{2 - q^2}{1 - q^2}) + B\xi^3, \quad \sum_{i=1}^{4} \mu_i p_i y_i^3 = A\eta q^{-2B} (B + \frac{1 - 2q^2}{1 - q^2}) + B\eta^3, \quad (33)$$

where  $A = a^B B q^2/(1-q^2)$ . Similar to eq. (30), these relations are exact only for  $\beta = 0$  and  $\beta = 1$ . However, numerical tests show that these formulae are accurate to  $\lesssim 1\%$  for other non-integer values of  $\beta$  (or B).

#### 2.5 The inclusion of an on-axis shear

The lens equation with an on-axis shear is given by

$$\xi = x + \gamma x - \frac{ax}{(x^2 + y^2/q^2)^{1-\beta/2}} \tag{34}$$

$$\eta = y - \gamma y - \frac{ayq^{-2}}{(x^2 + y^2/q^2)^{1-\beta/2}}$$
(35)

We can show that these equations can be transformed into equations (3) and (4) by a simple transformation. It can be easily verified that the transformation is given by

$$\xi' = \frac{\xi}{\sqrt{1+\gamma}} \qquad \eta' = \frac{\eta}{\sqrt{1-\gamma}} \tag{36}$$

$$x' = x\sqrt{1+\gamma} \qquad y' = y\sqrt{1-\gamma} \tag{37}$$

$$a' = a(1+\gamma)^{-\beta/2} \quad \beta' = \beta \quad q' = q\sqrt{\frac{1-\gamma}{1+\gamma}},$$
 (38)

where we denote the transformed quantities with a prime. Applying the above transformation, we obtain

$$\xi' = x' - \frac{a'x'}{(x'^2 + y'^2/q'^2)^{1-\beta'/2}},\tag{39}$$

$$\eta' = y' - \frac{a'y'q'^{-2}}{(x'^2 + y'^2/q'^2)^{1-\beta'/2}}. (40)$$

These are identical to eqs. (3) and (4) if we drop the prime.

The magnification transforms like

$$\mu_i' = \mu_i (1 - \gamma^2) \tag{41}$$

Now it is straightforward to generalize the moment relations (eqs. [30-33]) to the case with an on-axis shear by applying eqs. (36)-(41). In particular, for the zeroth and first moments we have

$$\sum_{i=1}^{4} \mu_i p_i = \frac{2}{(2-\beta)(1-\gamma^2)},\tag{42}$$

$$\sum_{i=1}^{4} \mu_i p_i x_i = \frac{2\xi}{(2-\beta)(1-\gamma^2)(1+\gamma)}, \quad \sum_{i=1}^{4} \mu_i p_i y_i = \frac{2\eta}{(2-\beta)(1-\gamma^2)(1-\gamma)}, \tag{43}$$

Notice that the inclusion of an on-axis shear changes the magnification relation (eq. [42]) only quadratically. It is straightforward but tedious to show that this relation holds even for an off-axis shear (cf. Dalal 1998). For the observed gravitational lenses, the external shear is usually between  $0 < \gamma < 0.3$  (Keeton, Kochanek & Seljak 1997), this would mean that for given slope of the elliptical power-law potential, the total sum of signed magnifications is known to within 10%.

Two interesting observations are worth making here. First, these simple formulae indicate that the moments of x (y) components  $\mathcal{M}_{x,n}$  of the images are only related to the  $\xi$  ( $\eta$ ) component of the source position. This seems remarkable since the magnification is in general a function of both  $\xi$  and  $\eta$ . Second, for an elliptical potential with an on-axis shear, we have

7 unknown quantities  $(\xi, \eta, a, q, \beta, \mu_1, \gamma)$  with 7 moment equations, so in principle we can use the moments to solve for the lens parameters directly. Indeed we have implemented such a routine. Unfortunately, using Monte Carlo simulations, we find that the results depend rather sensitively on the accuracy of image positions and flux ratios. The present observational uncertainties do not allow us to carry out such an exercise, although in the future such an effort may be more worthwhile in order to determine whether elliptical potentials provide adequate fits to the observed lenses. In any case, we will show next that the magnification relations do not hold exactly for the elliptical density distributions and therefore these relations should be used with some caution.

#### 3 SINGULAR ISOTHERMAL ELLIPTICAL DENSITY DISTRIBUTIONS

It is well known that power-law potentials develop unphysical features, such as dumb-bell shaped density contours or even negative densities, when the axial ratio is small (e.g., Kassi-ola & Kovner 1993). So it is important to check whether the relations derived for the simpler elliptical potentials are valid for the more realistic elliptical density distributions. Relations concerning only image positions seem to be equally well satisfied by the elliptical potentials and elliptical density distributions (Witt & Mao 1997). However, this is not necessarily true for the magnification relations since magnifications involve second order derivatives of the lensing potential rather than the first order for the image positions, and hence they could be more sensitive to the detailed potential forms. We show that indeed elliptical density and elliptical potentials have somewhat different magnification relations. In this paper, we focus on the singular elliptical density distribution (including an arbitrary shear) for two reasons: the first is that this model can reproduce the observed image configurations well, particularly the models incorporating a shear (Keeton, Kochanek & Seljak 1997). The second reason is that relatively little is known about the magnification properties for the elliptical density distributions, so a complete treatment of the general case is beyond the scope of this paper.

In polar coordinates  $(r, \theta)$ , the surface density for the singular isothermal distribution is given by

$$\kappa(r,\theta) = \frac{a}{2r} \frac{1}{(1 - \epsilon \cos 2\theta)^{1/2}},\tag{44}$$

where  $\epsilon = (1 - q^2)/(1 + q^2)$ , q is the axial ratio and a is again a characteristic radius that determines the overall image separations. For  $\epsilon > 0$ , the major axis is along the x-axis. The

lens equation (including a shear) is

$$\xi = (1+\gamma_1)x + \gamma_2 y - \frac{a}{\sqrt{2\epsilon}} \tan^{-1} \left[ \frac{\sqrt{2\epsilon} \cos \theta}{(1-\epsilon \cos 2\theta)^{1/2}} \right], \tag{45}$$

$$\eta = \gamma_2 x + (1 - \gamma_1) y - \frac{a}{\sqrt{2\epsilon}} \tanh^{-1} \left[ \frac{\sqrt{2\epsilon} \sin \theta}{(1 - \epsilon \cos 2\theta)^{1/2}} \right], \tag{46}$$

where  $(\gamma_1 = \gamma \cos 2\phi_s, \gamma_2 = \gamma \sin 2\phi_s)$  with  $\gamma$  being the strength of shear and  $\phi_s$  the "direction" of shear. The magnification for a given image is

$$(\det J)^{-1} = 1 - 2\kappa (1 + \gamma_1 \cos 2\theta + \gamma_2 \sin 2\theta) - \gamma^2. \tag{47}$$

These results can be found in Kormann et al. (1994) and Keeton & Kochanek (1998). Below we first discuss the simpler case without shear and then discuss some examples of the general case with shear (in an arbitrary direction).

## 3.1 The case without shear $(\gamma = 0)$

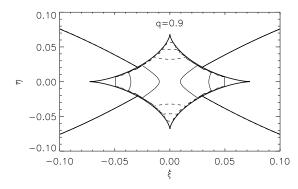
For this case, we have four (two) images if the source is inside (outside) a diamond-shaped caustic (see Fig. 1). Again, we study the sum of signed magnifications for the four image case. Recall that for an elliptical potential with the same power-law slope ( $\beta = 1$ ), the sum of signed magnification is exactly 2. Now for the isothermal elliptical density distribution, surprisingly, we find a value very close to 2.8, nearly independent of the ellipticity. For axial ratio in the range of 0.1 < q < 1, the sum of signed magnification varies little, from 2.65 to 2.8. This can be demonstrated by considering the special case where the source is located at the origin. The lens equation can be easily solved and the total signed magnification is given by

$$\sum_{i=1}^{4} \mu_i p_i = \frac{2}{1 - u/\tan^{-1} u} + \frac{2}{1 - v/\tanh^{-1} v},\tag{48}$$

where  $u = [2\epsilon/(1-\epsilon)]^{1/2}$  and  $v = [2\epsilon/(1+\epsilon)]^{1/2}$ . The above expression can be expanded in series around  $\epsilon = 0$ ,

$$\sum_{i=1}^{4} \mu_i p_i = \frac{14}{5} - \frac{32}{875} \epsilon^2 - \frac{490272}{21896875} \epsilon^4 + O[\epsilon^6]$$
(49)

The expansion only involves even powers of  $\epsilon$  and the coefficients are very small, which explain why the sum is nearly independent of  $\epsilon$  (or q). Numerically, we find that the sum varies  $\leq 10\%$  as long as we have four images, i.e., when the source is inside the caustics. To illustrate the near constancy of the sum of signed magnifications, we show in Fig. 1, the magnification contours for two values of q: a nearly spherical case with q = 0.9 and a



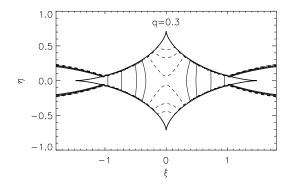


Figure 1. The left panel shows the contours for the sum of signed magnifications for q = 0.9. The axes are in units of a in eq. (44). The thick diamond-shaped curve is the caustic. The three dashed contours (from outer to inner) have magnifications 2.785, 2.79, and 2.795 respectively. The three solid contours (from inner to outer) have magnifications 2.8, 2.805 and 2.81, respectively. The outgoing contours from the cusp are those for two image configurations. The right panel is for q = 0.3. The dashed contour levels (from outer to inner) are 2.7, 2.725, and 2.75 respectively, while the four solid contour levels (from inner to outer) are 2.775, 2.8, 2.85, and 2.9, respectively. The outgoing contours (closely spaced together) from the cusp are contours for two image configurations. Notice the scales on the two axes are different.

fairly elongated case with q = 0.3; these values bracket the observed light axial ratios in early types of galaxies. The contour shapes are qualitatively the same; the case with q = 0.9 has a much smaller range in the total signed magnification (varies from  $\approx 2.79$  to  $\approx 2.82$ ) than the more elongated case. We emphasize that although the sum is nearly constant, it is quite different from the value (2) of the isothermal potential. This cautions against simple extrapolation of the magnification results obtained from elliptical potentials to elliptical density distributions.

#### 3.2 The case with shear

The lens equation with a shear is more complicated and can be studied only numerically. However, we find that for most cases, the sum of signed magnification is still around 2–3. In Fig. 2, we show one example for  $\gamma = 0.1$ ,  $\phi_s = 45^{\circ}$  and q = 0.8. For this set of parameters, the caustic structure is a deformed diamond, which divides the four image region (inside the diamond) and the two image region (outside the diamond). The sum of signed magnification at the origin is 2.47, while most areas inside the caustics have magnifications between 2.2 to 2.8.

However, there are significant exceptions to this. For some combinations of shear and ellipticity, the total signed magnification falls significantly outside the range of 2-3. The reason for this is that qualitatively different image configurations appear. More specifically, for some combinations of the  $\gamma$  and  $\epsilon$ , the caustics become small, and higher-order singularities (such as swallowtails) emerge. Fig. 3 shows how the caustics change for q = 0.6 when the

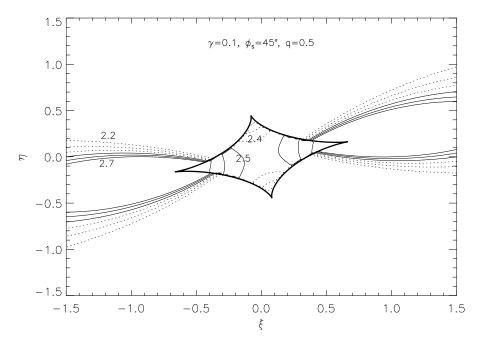


Figure 2. Contours for the sum of signed magnifications for q = 0.9,  $\gamma = 0.1$  and  $\phi_s = 45^{\circ}$ . The axes are in units of a in eq. (44). The thick diamond-shaped curve is the caustics. The three dotted contours have total magnifications 2.2, 2.3, and 2.4 respectively. The three solid contours have magnifications 2.5, 2.6 and 2.7, respectively. The outgoing lobes originating from the cusp are contours for two image configurations.

strength of shear changes but keep its angle fixed at  $\phi_s = 90^\circ$ . When the shear is  $\lesssim 0.1$ , the caustics form a diamond, similar to the case without shear. When the shear approaches a critical value ( $\approx 0.15$  for our case), swallowtails begin to develop, first along the y axis (see the top right panel), then along the x axis (lower right). For some intermediate shear value ( $\gamma = 0.165$ , lower left), complex caustics appear. Finally, when the shear becomes sufficiently large ( $\gtrsim 0.21$ ), the caustics (not shown) again covert to a simple diamond. For a source at the origin, the maximum number of images is eight, as can be seen for the case with  $\gamma = 0.165$  (lower left panel). For this case, the total signed magnification the four image configurations spans a considerable range, from  $\approx 0-20$  for various 4-image caustic regions. These values are considerably different from 2 found for the isothermal potential, or 2.8 for the isothermal elliptical density distribution without shear. The magnification for the central region with 8 images is approximately 5.06; this magnification does seem remarkably constant within 1% or so.

We have also checked for higher moments of the image positions weighted by the signed magnifications for the elliptical density distributions. We find that in general these moments no longer satisfy the simple relations we presented in §2, so we do not discuss these relations further.

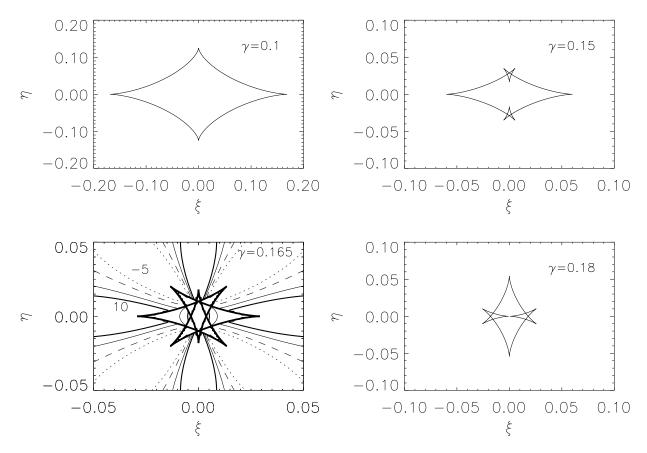


Figure 3. Caustic structures for an elliptical density distribution with q=0.6 and  $\phi_s=90^\circ$  as a function of the magnitude of shear  $\gamma$ . The axes are in units of a in eq. (44). The value of shear  $\gamma$  is indicated in each panel. Notice how swallowtail singularities appear and disappear as the shear changes. For  $\gamma \gtrsim 0.2$ , the caustics (not shown) are again a diamond, similar to the one shown at the top left, only elongated along the y-axis. For  $\gamma=0.165$ , the contours for the total signed magnification are shown for levels of 1.5 (dotted), 3 (dashed), 5.09 (thin solid), and 8 (thick solid). The thick complex-shaped curve is the caustic.

#### 4 SUMMARY AND DISCUSSION

In this paper, we have studied the elliptical potentials using a new moment approach. We have shown that the image positions weighted by signed magnifications satisfy fairly simple relations for this class of potentials. For example, the total signed magnifications is 2 for an isothermal elliptical potential, independent of the axial ratio (ellipticity); similarly simple results hold for higher moments. Our results confirm and extend those of Dalal (1998) on the power-law elliptical potentials. These results provide insights into the lensing properties of elliptical potentials. With improved image positions and flux ratios for lenses, the moment approach should allow us to understand more easily whether the power-law elliptical potentials can fit the observations data at all, without much numerical effort.

However, we also find that these relations do not hold for its cousin – the singular isothermal elliptical density distribution. For this elliptical density distribution without shear, the

#### 14 Witt & Mao

total signed magnification is 2.8, again nearly independent of the ellipticity, but significantly different from the value (2) for an isothermal potential. For the case with shear, the magnification relations become more complicated. For most cases we checked the total signed magnification is still around 2–3. However, the magnification no longer changes with the shear quadratically as in eq. (42), instead it is much more sensitive. There are also significant exceptions for the total signed magnification for some combinations of shear and ellipticity. The most striking feature is that 6 or 8 image configurations can occur (see Fig. 3). Notice, however, that the caustic structures are very small, so such image configurations may have too small cross-sections to be seen unless one observes a large number of quasars. This is likely to be true even after one takes into account the high magnification bias expected for these cases. Such cases, if discovered, will be easy to identify since the 6 or 8 images are located approximately on a circle.

The comparison between magnification relations in elliptical density distribution and elliptical potentials highlights the fact that magnifications are highly sensitive to the detailed form one uses for the lensing potential, much more so than the image positions; this is easily understood intuitively since magnifications involve higher order derivatives of the lensing potential which tend to amplify small differences in the parameters. Since even the more realistic elliptical density distribution is only an approximation for the real lensing potential, as evidenced by the twisted isophotes and many other irregular features in the light distribution, it is a reasonable extrapolation that the predicted magnifications from simple lens models can be significantly different from the observed ones. Indeed, for some radio lenses, one can show that even substructures with mass  $\geq 10^6 M_{\odot}$  can significantly influence the magnifications (Mao & Schneider 1998). It means that it will be difficult to model the flux ratios using simple lens models. However, this also means that with the steadily improving lens flux ratios and astrometries (e.g., see Blanton, Turner & Wambsganss 1998 for 2237+0305), we may be able to probe the structures in lensing galaxies in great detail and discriminate different classes of lensing potentials with confidence.

## ACKNOWLEDGMENTS

We thank Peter Schneider for helpful discussions and comments on the manuscript. This work was partially supported by the "Sonderforschungsbereich 375-95 für Astro-Teilchenphysik" der Deutschen Forschungsgemeinschaft.

#### REFERENCES

Binney J., Tremaine S., 1987, Galactic Dynamics, Princeton Univ. Press, Princeton, NJ

Blandford, R.D., Kochanek C.S., 1987, ApJ, 321, 658

Blanton M., Turner E.L., Wambsganss J. 1998, MNRAS, 298, 1223

Chang K., Refsdal S., 1979, Nature, 282, 561

Chae Y.-H., Khersonsky V.K., Turnshek D.A. 1998, ApJ, 506, 80

Dalal N., 1998, ApJ, 509, L13

Evans N.W., 1994, MNRAS, 267, 333

Kassiola A. Kovner, I., 1993, ApJ, 417, 450

Keeton II C.R., Kochanek C.S., 1998, ApJ, 495, 157

Keeton II C.R., Kochanek C.S., Seljak U., 1997, ApJ, 482, 604

Kochanek C.S., 1991, ApJ, 373, 354

Kochanek C.S., 1995, ApJ, 445, 559

Kormann R., Schneider P., & Bartelmann M., 1994, A&A, 284, 285

Hogg D.W., Blandford R.D., 1994, MNRAS, 268, 889

Mao S., Schneider P., 1998, MNRAS, 295, 587

Narayan R., Bartelmann M., 1998, Lectures on gravitational lensing, in Formation of structures in the universe, eds. A. Dekel J.P. Ostriker (Cambridge University Press)

Racine R., 1991, AJ, 102, 454

Rhie S. H., 1997, ApJ, 484, 63

Rix H.W., Schneider D.P., Bahcall, J.N., 1992, AJ, 104, 959

Schneider P., Ehlers J., Falco E. E., 1992, Gravitational Lenses (Springer-Verlag: New York)

Walsh D., Carswell R. F., Weymann R. J., 1979, Nature, 279, 381

Wambsganss J. Paczyński B., 1994, AJ, 108, 1156

Witt H.J., 1996, ApJ, 472, L1

Witt H.J., Mao S., 1995, ApJ, 447, L105

Witt H.J., Mao S., 1997, MNRAS, 291, 211

Witt H.J., Mao S., & Schechter P. L. 1995, ApJ, 443, 18

Yee H.K.C., 1988, AJ, 95, 1331

## 16 Witt & Mao

This paper has been produced using the Royal Astronomical Society/Blackwell Science  $\LaTeX$  style file.